Organochlorides Mediate Oxidation Reactions Induced by Low Dose Ionizing Radiation

Liu, Juncheng; Brevé, Tobias G.; Xu, Bing; Hagedoorn, Peter Leon; Denkova, Antonia G.; Eelkema, Rienk

DOI
10.31635/ccschem.024.202303794

Publication date
2024

Document Version
Final published version

Published in
CCS Chemistry

CCS Chemistry

RESEARCH ARTICLE

Received: Dec. 21, 2023 | Accepted: Feb. 23, 2024 | Published: Mar. 23, 2024

Organochlorides Mediate Oxidation Reactions Induced by Low Dose Ionizing Radiation

Juncheng Liu[1], Tobias G. Brevé[2], Bing Xu[1], Peter-Leon Hagedoorn[3], Antonia G. Denkova[1]* & Rienk Eelkema[2]*

[1]*Department of Radiation Science and Technology, Delft University of Technology, 2629 JB Delft,* [2]*Department of Chemical Engineering, Delft University of Technology, 2629 HZ Delft,* [3]*Department of Biotechnology, Delft University of Technology, 2629 HZ Delft*

**Corresponding authors: A.G.Denkova@tudelft.nl; R.Eelkema@tudelft.nl*

Cite this: *CCS Chem.* **2024**, 6, 1712–1720
DOI: 10.31635/ccschem.024.202303794

The controlled release of drugs using local ionizing radiation presents a promising approach for targeted cancer treatment, particularly when applied in concurrent radio-chemotherapy. In these approaches, radiation-generated reactive species often play an important role. However, the reactive species that can be used to trigger release have low yield and lack selectivity. Here, we demonstrate the generation of highly oxidative species when aqueous solutions containing low concentrations of organochlorides (such as chloroform) are irradiated with ionizing radiation at therapeutically relevant doses. These reactive species were identified as peroxyl radicals, which formed in a reaction cascade between organochlorides and aqueous electrons. We employed stilbene-based probes to investigate the oxidation process, showing double bond oxidation and cleavage. To translate this reactivity into a radiation-sensitive material, we synthesized a micelle-forming amphiphilic block copolymer that has stilbene as the linker between two blocks. Upon exposure to ionizing radiation, the oxidation of stilbene led to the cleavage of the polymer, which induces the dissociation of the block-copolymer micelles and the release of loaded drugs.

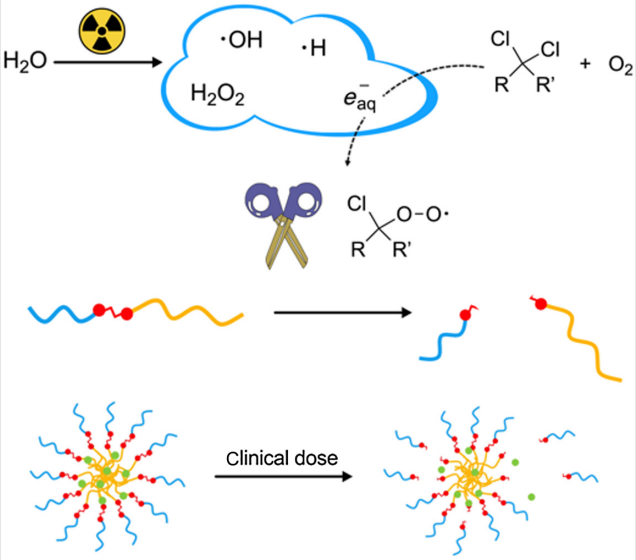

Keywords: drug delivery, micelles, radiation chemistry, reactive oxygen species, ionizing radiation, reaction mechanisms

Introduction

Over the last few decades, smart materials that exhibit responses to various stimuli have found wide application in drug delivery systems.[1,2] In the area of cancer treatment, stimuli-responsive self-assemblies composed of amphiphilic block copolymers are used to encapsulate hydrophobic antitumor drugs to transport them in the bloodstream, which helps to address the challenge of poor solubility and also mitigates the toxic effects of the

DOI: 10.31635/ccschem.024.202303794
Citation: *CCS Chem.* **2024**, 6, 1712–1720
Link to VoR: https://doi.org/10.31635/ccschem.024.202303794

drugs.[3,4] Several biodegradable polymer building blocks, including poly(ε-caprolactone) (PCL), poly(lactide-co-glycolide),[5] and polyethylene glycol (PEG), have been approved by the U.S. Food and Drug Administration for clinical application.[6] These polymers can be modified such that they exhibit changes in physical or chemical properties upon exposure to stimuli from external sources (e.g., light,[7] ultrasound,[8] and magnetic field[9]) or from cancerous tissues (e.g., pH,[10] reactive oxygen species,[11,12] temperature,[9] and biomarkers[13]). These changes can include alterations in their aggregation state or bond cleavage, which in turn facilitate controlled drug release in tumor cells.

Among the various stimuli of interest, ionizing radiation is a promising external stimulus owing to its capability of precise and deep tissue penetration.[14–17] Combined radiotherapy and chemotherapy has been demonstrated to exhibit improved therapeutic efficacy in the treatment of cancer.[18–21] In biological systems, the exposure to ionizing radiation initiates a cascade of reactions which result in the generation of reactive species including aqueous electrons, hydroxyl radicals, hydrogen radicals, and hydrogen peroxide. These species have been shown to trigger reactions that lead to bond cleavage and subsequent release of drugs. For example, the oxidative cleavage of diselenide bonds by hydroxyl radicals results in the disassembly of diselenide-based nanoparticles, facilitating the release of encapsulated drugs.[22–24] Radiation-responsive groups have been applied in prodrug therapy,[25–28] wherein an antitumor drug is protected and can be selectively activated upon reacting with hydroxyl radicals or aqueous electrons. The applied radiation dose should be within the clinically relevant window, which depends on the specific type of radiotherapy. For instance, in external beam radiotherapy, patients typically receive a dose fraction of 1.8–2 Gy over 6–7 weeks, accumulating to a total dose of 60–70 Gy,[29–31] while in radioembolization higher doses (80–100 Gy) are applied.[32] In radionuclide therapy, localized doses as high as 100 Gy can be achieved.[33] Despite the success in applying radiation-responsive functional groups, the studies of smart materials that exhibit response to ionizing radiation, especially clinically relevant doses, is still limited due to the poor sensitivity and selectivity when used to trigger reactions.

Herein, we present the discovery of an ionizing radiation-induced oxidation reaction that is greatly amplified in the presence of low concentrations of aliphatic organochlorides. This amplification effect is attributed to the generation of aliphatic peroxyl radicals, which arise from the reaction between the organochlorides and radiation-generated aqueous electrons (Figure 1a). Stilbene serves as a suitable probe for monitoring the oxidation process, as it undergoes oxidation specifically at its double bond motif, resulting in a measurable decrease in UV–vis light absorption. Subsequently, we have developed a stilbene-linked amphiphilic block copolymer (poly(ε-caprolactone)-stilbene-poly(ethylene glycol) (**PSP**)) that allows for radiation-induced release of a chemotherapeutic drug.

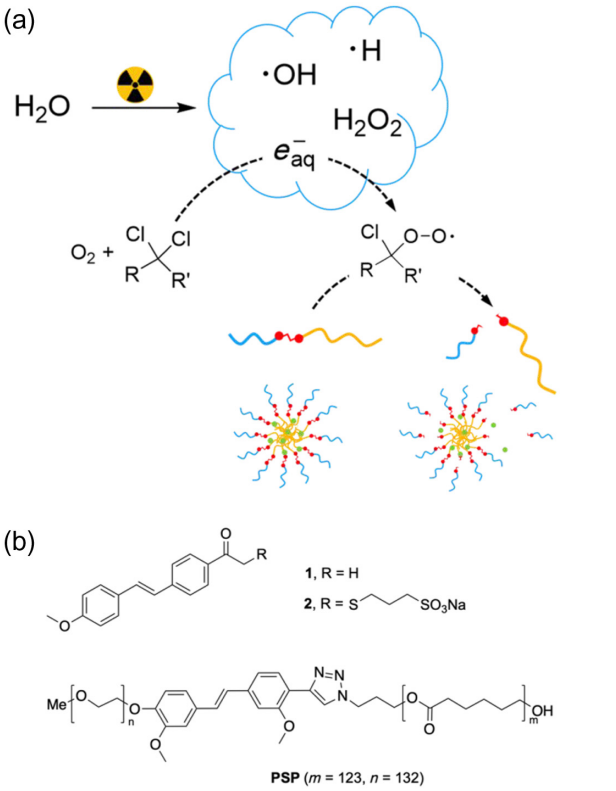

Figure 1 | *Oxidative cleavage of stilbene by radiation in water containing organochloride. (a) Proposed sequence of events; (b) chemical structure of compound **1**, **2** and block copolymer **PSP**.*

Experimental Methods

All compounds were purchased from commercial suppliers (Sigma Aldrich (Zwijndrecht, the Netherlands), Tokyo Chemical Industry (Zwijndrecht, the Netherlands) and abcr Gute Chemie (Karlsruhe, Germany)) and used without further purification unless otherwise specified. Compound **S3** was synthesized according to previous work from our group.[34] Detailed synthesis procedures of compounds **1**, **2** and polymer **PSP** are presented in the Supporting Information. Reactions were monitored by thin-layer chromatography on a silica gel plate and visualized by UV light (254 nm) or stained using a $KMnO_4$/OH^- solution. Flash column chromatography was carried out on a 30 cm column loaded with 230–400 mesh silica gel. ^{1}H-NMR spectra were recorded on an Agilent-400 MR DD2 (Santa Clara, United States) (399.67 MHz) at 298 K. UV–vis spectroscopic measurements were performed on an Analytik Jena Specord spectrometer (Unterschleißheim, Germany). Milli-Q water was obtained

DOI: 10.31635/ccschem.024.202303794
Citation: *CCS Chem.* **2024**, 6, 1712–1720
Link to VoR: https://doi.org/10.31635/ccschem.024.202303794

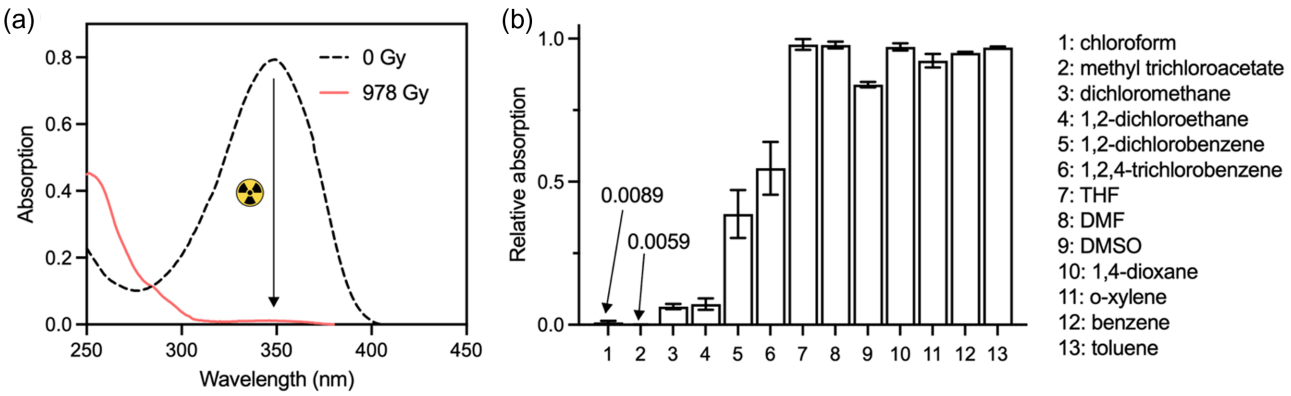

Figure 2 | *(a) UV–vis absorption of compound **1** before and after 978 Gy of γ-irradiation in chloroform. (b) Relative absorption of compound **1** after 978 Gy of γ-irradiation in different solvents. The γ-rays are delivered by the ^{60}Co source, absorption is relative to the unirradiated solution. Error bars represent experimental uncertainties of three samples.*

by purification of demineralized water with a Milli-Q IQ 7000 (Darmstadt, Germany) machine equipped with a Millipak 0.22 μM filter. High-performance liquid chromatography–mass spectrometry (HPLC-MS) was performed on a LTQ XL spectrometer from Thermo Scientific (Bleiswijk, The Netherlands) that was connected with a Shimadzu HPLC setup with D2 detector and Discovery C18 reverse phase column (Kyoto, Japan). Water/MeCN with 0.1% (v/v) formic acid was used as the mobile phase at a flow rate of 0.2 mL/min. The average molecular weight and dispersity ($Đ$, M_w/M_n) of the synthesized polymers were determined using a Shimadzu gel permeation chromatography (GPC) (Kyoto, Japan) system, which was equipped with a Shimadzu RID-10A refractive index detector and a Shimadzu SPD-20A UV–vis detector. Two columns, a PL gel guard column (MIXED-C, 5 μm) with dimensions of 50 mm × 7.5 mm and an Agilent PLGel (Santa Clara, United States) (MIXED-C, 5 μm) column with dimensions of 300 mm × 7.5 mm, were used. The GPC system provided an effective molar mass range of 200 to 2 × 10^6 g/mol. The eluent used was *N,N*-dimethylformamide LiBr (25 mM), and the flow rate was set to 1.0 mL/min. The measurements were conducted at a temperature of 50 °C. The GPC was calibrated with low dispersity PEG standards (Sigma Aldrich) from 200 to 200,000 g/mol. Dynamic light scattering (DLS) was performed on a Malvern Pananalytical Zetasizer Pro (Worcestershire, United Kingdom) equipped with laser operating at 633 nm. The irradiations with γ-rays were performed using a Nordion 220 ^{60}Co gamma cell (Ottawa, Canada). The dose rate at the experimental date was around 460 Gy/h which is calculated based on the decay law and the half-life of ^{60}Co. The delivered dose was calculated by the dose rate at the date of the experiments multiplied by the exposure time. Radiation was given in one fraction unless otherwise specified. The X-ray irradiation was carried out using an X-ray source (Philips MCN 321 variable-energy X-ray tube, Eindhoven, The Netherlands) performed in a working voltage of 240 keV and a current of 10 mA. The dose rate of the X-ray source was determined using the method as described in literature.[35]

Results and Discussion

We recently found that the absorbance of a chloroform solution of the trans-stilbene derivative **1** decreased after exposure to γ-rays from a ^{60}Co source (Figure 2a). The *vic*-diol as well as 4-acetylbenzaldehyde and 4-anisaldehyde were identified as products indicating oxidation and oxidative cleavage of the ethene moiety in compound **1** (Supporting Information Figures S3–S5, Scheme S1). Given that the concentration of compound **1** is 50 μM in chloroform, it is unlikely that compound **1** undergoes direct radiation-induced oxidation reactions. Rather, it is more plausible that interaction of chloroform, the solvent, with ionizing radiation generates reactive species that subsequently oxidize compound **1**. Previous research by Wilhelm and coworkers.[36] reported the formation of Cl_2 and CCl_3OOH during γ-irradiation of O_2-saturated chloroform. Given this precedent and the products identified from the reaction of **1**, we propose that compound **1** is oxidized by a peroxide species generated during radiolysis of chloroform.

To investigate the influence of the solvent on the radiolysis of stilbene, compound **1** was dissolved in various solvents and subsequently exposed to γ-radiation. We employed the relative UV–vis light absorption to evaluate the extent of decomposition (Figure 2b). The relative absorption is calculated from the absorption of compound **1** at 350 nm postirradiation divided by its initial absorption. Interestingly, oxidation occurs in all tested chlorinated organic solvents, whereas in non-chlorinated solvents, the molecule remains intact after

DOI: 10.31635/ccschem.024.202303794
Citation: *CCS Chem.* **2024**, 6, 1712–1720
Link to VoR: https://doi.org/10.31635/ccschem.024.202303794

irradiation. We therefore concluded that the carbon-chlorine bond plays a crucial role in the oxidation of stilbene during radiolysis. Furthermore, the extent of decomposition varies depending on the solvent used. Chloroform and methyl trichloroacetate, where a carbon atom is bonded to three chlorine atoms, showed the largest effect. In 1,2-dichloroethane and dichloromethane, where a carbon atom is bonded to fewer than three chlorine atoms, a lower degree of oxidation is observed. In contrast, for chlorinated aromatic solvents such as 1,2-dichlorobenzene and 1,2,4-trichlorobenzene, compound **1** exhibits the lowest degree of oxidation among all chlorine-based solvents. According to previous research conducted by Packer et al.,[37] the reactivity of alkyl peroxyl radicals increases when the α-carbon is bonded with chlorine, with further enhancement observed upon multiple chlorine substitutions. These trends align with our observations.

To test if this organochloride-mediated radiolysis of stilbene could take place in water, we synthesized compound **2** (Figure 1b), in which a sulfonate group was introduced to increase solubility in water. Upon irradiation by γ-rays (75 Gy) in water, the concentration of compound **2** decreased from 90 μM to 56 ± 0.2 μM, indicating its oxidation (Supporting Information Figure S6). Only diol (compound **S11** in Supporting Information Scheme S2 and Figure S7c) was identified as the product of radiolysis under these conditions. When 0.1 vol % chloroform was added in the solution (the maximum solubility of chloroform in water at 20 °C is 0.54 vol % according to the International Union for Pure and Applied Chemistry-National Institute of Standards and Technology (IUPAC-NIST) database), a greater decrease was observed (from 90 μM to 28.1 ± 1.0 μM) after exposure to the same dose of radiation. This indicates the involvement of additional reactive species derived from the radiolysis of chloroform. The corresponding aldehyde (compound **S12** and *p*-anisaldehyde) and diol (compound **S11**) were found in MS, suggesting a further oxidating process compared to pure water.

Inspired by the ionizing radiation-induced oxidative cleavage of stilbene, we aimed to design a radiation-responsive nanocarrier capable of dissociating upon exposure to radiation. For this purpose, we have synthesized an amphiphilic block copolymer, **PSP**, using a stilbene derivative as the linker connecting the hydrophilic and hydrophobic blocks (Figure 1b). We chose PCL and PEG as the polymer blocks since they are widely employed materials for nanocarriers in biomedical settings.

To verify the radiation-induced cleavage of **PSP**, we prepared micelles and irradiated the solutions with γ-rays over a dose range of 0–8 Gy, using phosphate-buffered saline (PBS, pH 7.4) or PBS/chloroform (0.1 vol % chloroform in PBS, pH 7.4) as the solvent. We employed X-rays (240 keV) as an alternative irradiation source. We used fractionated radiation of 2 Gy per fraction, since these conditions are close to clinical application. The micelle solution exhibits an absorption peak at 350 nm, corresponding to the absorption of the stilbene moiety in **PSP** (Supporting Information Figure S9). Figure 3a shows a significant decrease of absorption after 4 Gy of irradiation in PBS/chloroform. The gradual decrease indicates a dose-dependent oxidation of stilbene. However, irradiation with the same dose in PBS leads to a much less pronounced decrease in absorption and no change in the peak shape (Supporting Information Figure S9), indicating no oxidation in the absence of chloroform. The energy of the irradiation source does not significantly influence the efficiency of the oxidation process, as evidenced by the similar slopes of absorption decrease observed for X-rays and γ-rays. This phenomenon should be similar to chemical reactions triggered by species formed when exposed to radiation having the same linear energy transfer value since the yield of each primary species, described by its G-value (molecules produced per 100 eV absorbed energy) will be nearly the same.

We varied the concentration of chloroform in PBS to investigate the effect of the molar ratio of chloroform-to-stilbene on the oxidation process. The extent of the decrease in absorption correlates with the chloroform-to-stilbene ratio (Figure 3b). At the molar ratio of 500:1, the absorption decreases from 1.0 to 0.60, whereas at molar ratios ranging from 10:1 to 0.5:1, the absorption does not decrease. The dependence indicates that the oxidation is not catalytic in nature but rather requires an excess amount of chloroform.

We lyophilized the micelle solutions after irradiation and measured the molecular weight of the polymers using GPC to verify the oxidative cleavage of **PSP**. As shown in Figure 3c, **PSP** has a retention time of 8.19 min, correspond to a molecular weight of 9.3 kDa. Following the exposure to 15 Gy of γ-irradiation in the presence of chloroform, a shoulder peak appears at a retention time of 8.44 min, which is the same retention time as the PCL-block. A higher exposure dose of 30 Gy increases the intensity of the PCL peak, further supporting the conclusion that the oxidative cleavage by radiation is dose dependent.

The oxidation pathway of stilbene varies depending on the solvent, as the irradiated medium generating reactive species is different. In chloroform, the oxidizing agents generated through the radiolysis of chloroform include Cl_2 and CCl_3OOH.[36] However, in aqueous solutions, the majority of ionizing radiation energy is absorbed by water molecules, leading to the generation of primary species such as aqueous electrons (e_{aq}^-), hydroxyl radicals ($OH\cdot$) and hydrogen radicals ($H\cdot$) (eq 1). Experimental studies using pulse radiolysis[38–42] have confirmed that in the presence of chloroform, the primary reaction of chloroform involves reduction by e_{aq}^- because of the high electron affinity, resulting in the formation of chloride ions and the carbon-centered radical $\cdot CHCl_2$ (eq 2). In the presence of trace amount of oxygen, the $\cdot CHCl_2$

DOI: 10.31635/ccschem.024.202303794
Citation: *CCS Chem.* **2024**, 6, 1712–1720
Link to VoR: https://doi.org/10.31635/ccschem.024.202303794

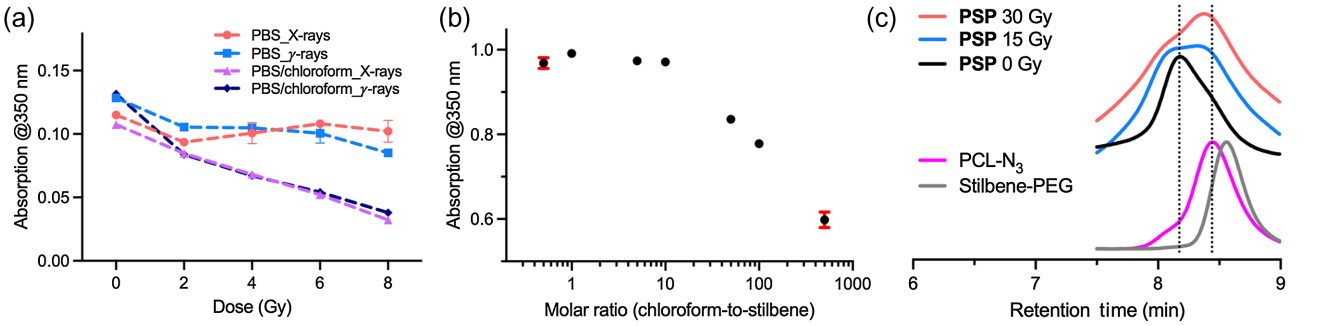

Figure 3 | *(a) Decrease of the absorption of **PSP** micelle solutions (0.05 mg/mL) at 350 nm against radiation dose; (b) decrease of absorption after 75 Gy of irradiation in solutions with varied chloroform-to-stilbene ratio (for some data, error bars are smaller than data markers); (c) GPC retention time of PCL-block, PEG-block, **PSP** before and after γ-irradiation in water/0.1 vol % chloroform solution. The γ-rays are delivered by the ^{60}Co source. We used 240 keV X-rays. Error bars represent experimental uncertainties of three samples.*

reacts with oxygen at a diffusion-controlled rate, leading to the formation of peroxyl radicals (eq 3) that are able to oxidize stilbene.

$$H_2O \xrightarrow{\gamma\text{-rays}} H\cdot + HO\cdot + e^-_{aq} + H^+ \quad (1)$$

$$CHCl_3 + e^-_{aq} \rightarrow \cdot CHCl_2 + Cl^- \quad (2)$$

$$\cdot CHCl_2 + O_2 \rightarrow Cl_2HCOO\cdot \quad (3)$$

We conducted scavenger experiments to investigate the underlying mechanism of radiation-induced stilbene oxidation in water/0.1 vol % chloroform solution. Micelle solutions were irradiated in PBS (pH 7.4) containing 0.1 vol % chloroform and scavengers. Irradiation of the micelle solution in a PBS buffer yields negligible absorption reduction (96.0% remaining), whereas the addition of 0.1 vol % chloroform results in a notable reduction to 38.9% (Figure 4a). The presence of 10 mM tert-butanol (·OH scavenger) leads to no significant difference in absorption reduction compared to that of the chloroform experiment (P = 0.17), suggesting that scavenging of the hydroxyl radical does not impede the reaction. Scavenging of the peroxyl radical by 10 mM ascorbic acid or of aqueous electrons by 100 mM $NaNO_3$ shows much less absorption reduction than the chloroform experiment, which means the peroxyl radical and aqueous electrons

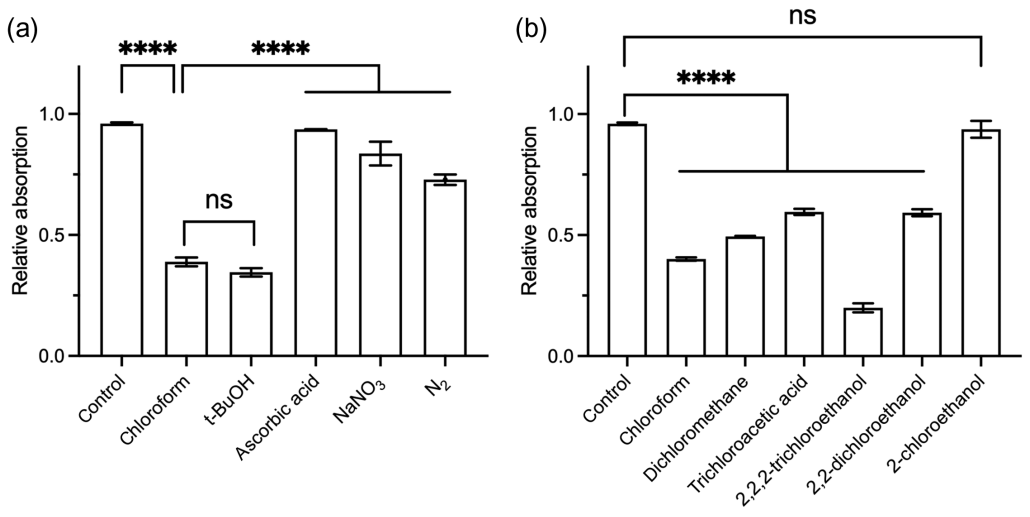

Figure 4 | *(a) The relative absorption of micelles solutions with scavengers after 75 Gy of γ-irradiation. Control, 0.5 mg/mL **PSP** in 10 mM PBS (pH 7.4); chloroform, 0.1 vol % chloroform was added to the control solution. Scavengers were added to the 0.1 vol % chloroform solution:* t-BuOH, *10 mM; ascorbic acid, 10 mM; $NaNO_3$, 100 mM. N_2, solution was degassed and backfilled with N_2 before adding chloroform. (*n *= 3, one-way analysis of variance (ANOVA)* t-test, P-*values >0.05 show as "ns," **** indicates* P-*value < 0.0001). (b) The relative absorption of micelle solutions containing 12 mM organochlorides after 75 Gy of γ-irradiation. Control, 0.5 mg/mL **PSP** in 10 mM PBS (pH 7.4). Organochloride samples were generated by adding the respective organochloride to the control solution.*

DOI: 10.31635/ccschem.024.202303794
Citation: *CCS Chem.* **2024**, 6, 1712–1720
Link to VoR: https://doi.org/10.31635/ccschem.024.202303794

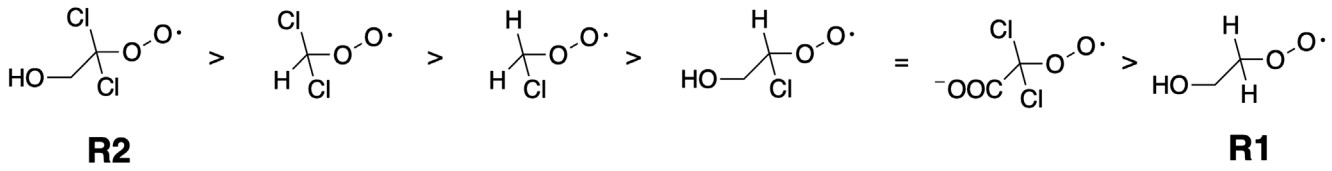

Scheme 1 | *Relative reactivity towards stilbene.*

must play a role in the reaction. Removal of oxygen via nitrogen purging results in an absorption reduction to 73% of the original value, suggesting the participation of oxygen in the oxidation. Additional electron paramagnetic resonance experiments using spin traps showed the formation of hydrated electrons under γ-irradiation of PBS, and their efficient removal in the presence of chloroform (see Supporting Information Figure S11, Scheme S3, and Table S1). These findings provide further confirmation that the oxidation of stilbene is associated with aqueous electron and peroxyl radical formation during the radiolysis of aqueous solutions containing chlorinated compound.

We investigated whether chlorinated organic molecules, apart from chloroform, can induce oxidation of stilbene under irradiation. Micelle solutions containing various chlorinated molecules at equal concentration (12 mM, equal to that of 0.1 vol % chloroform in PBS) were irradiated with the same dose of γ-rays, and the degree of oxidation was evaluated based on the reduction in absorption. Note that all used organochlorides are added at concentrations below their solubility limit in water, that is, in all cases homogenous solutions were used. As illustrated in Figure 4b, all multichlorinated organic additives exhibit oxidizing capabilities, whereas the monochlorinated 2-chloroethanol shows no significant difference in reduction compared to that observed in PBS alone. This suggests that the peroxyl radical formed from 2-chloroethanol (**R1**, Scheme 1) lacks sufficient reactivity to react with stilbene. In contrast, **R2**, formed from 2,2,2-trichloroethanol, shows the highest reactivity among all tested molecules, resulting in an absorption decrease of 80%. This can be attributed to the electron-withdrawing effect of the chlorine and hydroxyl groups, which render the corresponding peroxyl radical more reactive. The same trend is observed in experiments involving chloroform and dichloromethane. At the pH of these experiments, trichloroacetic acid and the so formed peroxyl radicals are ionized. The carboxylate ion group exhibits a deactivating effect, as previously reported by Packer et al.,[37] so the degree of oxidation in trichloroacetic acid is lower compared to that in the chloroform experiment.

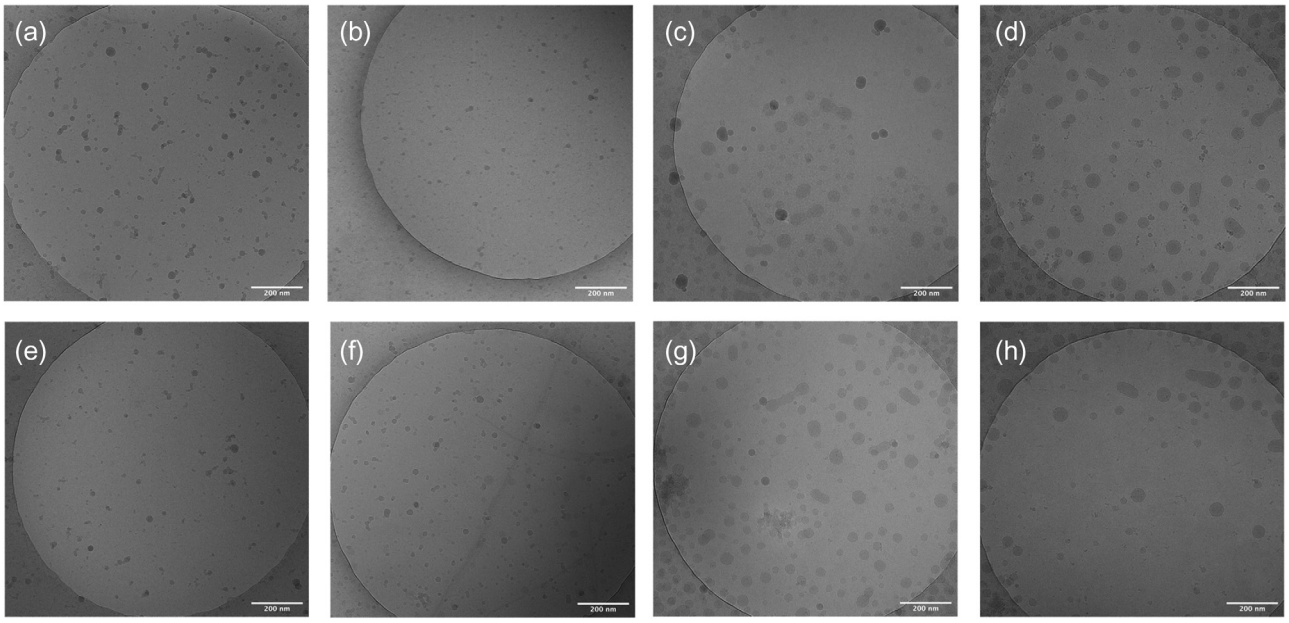

Figure 5 | *Cryo-EM images of **PSP** micelles and **PSP**-encapsulating Dox. (a) **PSP** micelle solution in water, 0 Gy; (b) **PSP** micelle solution in water/chloroform, 0 Gy; (c) **PSP**-Dox micelle solution in water, 0 Gy; (d) **PSP**-Dox micelle solution in water/chloroform, 0 Gy; (e) **PSP** micelle solution in water, 15 Gy; (f) **PSP** micelle solution in water/chloroform, 15 Gy; (g) **PSP**-Dox micelle solution in water, 15 Gy; (h) **PSP**-Dox micelle solution in water/chloroform, 15 Gy.*

DOI: 10.31635/ccschem.024.202303794
Citation: *CCS Chem.* **2024**, 6, 1712–1720
Link to VoR: https://doi.org/10.31635/ccschem.024.202303794

Cryo-EM images were used to investigate the morphological changes of the micelles after irradiation in water or water/0.1 vol % chloroform solution. As shown in Figure 5a,b, the nonirradiated samples exhibit predominantly spherical particles, with a minor presence of worm-like structures. Particle analysis of the nonirradiated micelles showed an average core diameter of 16.3 ± 4.9 nm in water and 14.7 ± 3.0 nm in water/chloroform (Supporting Information Figure S10). Upon exposure to 15 Gy of γ-radiation, the micelles maintained their spherical morphology (Figure 5e,f), with an average core diameter of 16.1 ± 3.6 nm in water and 14.4 ± 4.1 nm in water/chloroform. The size distribution of the micelles before and after irradiation in water or in water/chloroform exhibited minimal variation, indicating that the structure of the micelles was preserved. The hydrodynamic diameter (D_H) of **PSP**, determined by DLS, exhibited no size distribution shift after irradiation in water and water/chloroform (Supporting Information Figure S10a,d).

To test the drug release property of **PSP** micelles under irradiation, we used doxorubicin (Dox) as a model drug. The Dox loading efficiency in the micelles was 0.23–0.25 mg/mg (Dox/**PSP**). **PSP**-Dox micelles showed significantly larger core diameter than **PSP** micelles (cryogenic electron microscopy (cryo-EM): 36.2 ± 10.7 nm in water and 43.9 ± 10.1 nm in water/chloroform, Figure 5c,d). The D_H (DLS) of Dox-loaded micelles was 97.8 ± 1.0 nm, while that of unloaded micelles was 38.2 ± 0.2 nm (Supporting Information Figure S13 and Table S3). The relatively larger diameter of **PSP-Dox** compared to **PSP** alone is attributed to the high Dox loading in the hydrophobic core of the micelles. Upon exposure to 15 Gy of γ-irradiation in water/chloroform, cryo-EM of **PSP**-Dox showed a lower number of large micelles (40–55 nm) and relatively more small micelles (15–30 nm) (Figure 5d,h and Supporting Information Figure S10k,l). In contrast, **PSP**-Dox micelles in water exhibited no significant change of morphology when irradiated by γ-rays (cryo-EM: Figure 5c,g and Supporting Information Figure S10h,i).

The Dox release ratio after irradiation was determined, representing the releasing Dox from the micelles divided by the total Dox after irradiation. As shown in Figure 6, both groups exhibited a Dox release of approximately 30% at 0 Gy, indicating a passive release of Dox during the preparation of the micelle solutions. After 8 Gy of irradiation, there was no significant difference in Dox release between the PBS and PBS/chloroform group. However, an increase in radiation dose to 15 Gy, resulted in a higher release of Dox in the PBS/chloroform group, that is, a release of 74.4%, while in the PBS group 45.7% released from the micelles. Increasing the exposure dose to 30 Gy showed the same trend as observed in the 15 Gy case.

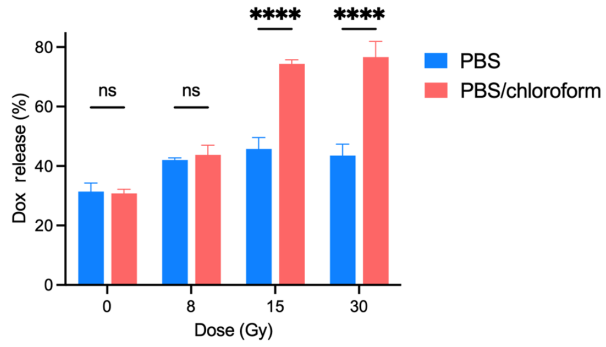

Figure 6 | *The release profiles of Dox from **PSP** micelles solutions irradiated in PBS and PBS/chloroform solution (n = 3, two-way ANOVA t-test, **** indicates P-value < 0.0001).*

Conclusion

We show that the presence of low concentration organochloride compounds can have a profound effect on the oxidizing capabilities of reactive species generated in the radiolysis of water. Using clinical dose gamma rays or X-rays, we observed oxidative cleavage of stilbene derivatives in buffered aqueous solutions containing 0.1 vol % chloroform or other multichloro compounds. Mechanistic studies revealed that the reactive species responsible for the oxidation reaction were peroxyl radicals generated through the reaction between aqueous electrons and chlorinated molecules. Irradiation of micelles, composed of an amphiphilic block copolymer with stilbene serving as the linkage between the two building blocks, in a water/0.1 vol % chloroform solution, resulted in the breakage of polymer chains. This, in turn, led to the disruption of the micelles and the subsequent release of the cargo encapsulated within them. This study offers valuable insights into the molecular design of radiation-sensitive materials intended for use in controlled drug delivery applications, in particular for combined chemotherapy and radiotherapy. As the application of small molecular organochlorides in clinical settings poses biocompatibility concerns, we are currently investigating avenues to reduce organochloride toxicity.

Supporting Information

Supporting Information is available and includes experimental details on the synthesis of compound **1**, **2** and polymer **PSP**; Figures S1–S14; Schemes S1–S3; and Tables S1–S3.

Conflict of Interest

There is no conflict of interest to report.

DOI: 10.31635/ccschem.024.202303794
Citation: *CCS Chem.* **2024**, 6, 1712–1720
Link to VoR: https://doi.org/10.31635/ccschem.024.202303794

Funding Information

This work has received funding from the Chinese Scholarship Council (J.L.) and the European Research Council (R.E., ERC Consolidator Grant 726381).

Acknowledgments

The authors wish to acknowledge Dr. Wiel Evers for conducting the cryo-EM measurements and Dr. Robin de Kruijff for discussion on the cryo-EM images.

References

1. Cao, Z. Q.; Wang, G. J. Multi-Stimuli-Responsive Polymer Materials: Particles, Films, and Bulk Gels. *Chem. Rec.* **2016**, *16*, 1398–1435.
2. Criado-Gonzalez, M.; Mecerreyes, D. Thioether-Based ROS Responsive Polymers for Biomedical Applications. *J. Mater. Chem. B* **2022**, *10*, 7206–7221.
3. Ge, Z.; Liu, S. Functional Block Copolymer Assemblies Responsive to Tumor and Intracellular Microenvironments for Site-Specific Drug Delivery and Enhanced Imaging Performance. *Chem. Soc. Rev.* **2013**, *42*, 7289–7325.
4. Lv, S.; Wu, Y.; Cai, K.; He, H.; Li, Y.; Lan, M.; Chen, X.; Cheng, J.; Yin, L. High Drug Loading and Sub-Quantitative Loading Efficiency of Polymeric Micelles Driven by Donor-Receptor Coordination Interactions. *J. Am. Chem. Soc.* **2018**, *140*, 1235–1238.
5. Bawa, K. K.; Oh, J. K. Stimulus-Responsive Degradable Polylactide-Based Block Copolymer Nanoassemblies for Controlled/Enhanced Drug Delivery. *Mol. Pharm.* **2017**, *14*, 2460–2474.
6. Bobo, D.; Robinson, K. J.; Islam, J.; Thurecht, K. J.; Corrie, S. R. Nanoparticle-Based Medicines: A Review of FDA-Approved Materials and Clinical Trials to Date. *Pharm. Res.* **2016**, *33*, 2373–2387.
7. Men, Y.; Breve, T. G.; Liu, H.; Denkova, A. G.; Eelkema, R. Photo Cleavable Thioacetal Block Copolymers for Controlled Release. *Polym. Chem.* **2021**, *12*, 3612–3618.
8. Wei, P.; Cornel, E. J.; Du, J. Ultrasound-Responsive Polymer-Based Drug Delivery Systems. *Drug Deliv. Transl. Res.* **2021**, *11*, 1323–1339.
9. Zou, H.; Yuan, W. Temperature- and Redox-Responsive Magnetic Complex Micelles for Controlled Drug Release. *J. Mater. Chem. B* **2015**, *3*, 260–269.
10. Mao, J.; Li, Y.; Wu, T.; Yuan, C.; Zeng, B.; Xu, Y.; Dai, L. A Simple Dual-pH Responsive Prodrug-Based Polymeric Micelles for Drug Delivery. *ACS Appl. Mater. Interfaces* **2016**, *8*, 17109–17117.
11. Piergentili, I.; Bouwmans, P. R.; Reinalda, L.; Lewis, R. W.; Klemm, B.; Liu, H.; de Kruijff, R. M.; Denkova, A. G.; Eelkema, R. Thioanisole Ester Based Logic Gate Cascade to Control ROS-Triggered Micellar Degradation. *Polym. Chem.* **2022**, *13*, 2383–2390.
12. Sun, C.; Liang, Y.; Hao, N.; Xu, L.; Cheng, F.; Su, T.; Cao, J.; Gao, W.; Pu, Y.; He, B. A ROS-Responsive Polymeric Micelle with a pi-Conjugated Thioketal Moiety for Enhanced Drug Loading and Efficient Drug Delivery. *Org. Biomol. Chem.* **2017**, *15*, 9176–9185.
13. Ding, Y.; Kang, Y.; Zhang, X. Enzyme-Responsive Polymer Assemblies Constructed Through Covalent Synthesis and Supramolecular Strategy. *Chem. Commun.* **2015**, *51*, 996–1003.
14. Liu, H.; Laan, A. C.; Plomp, J.; Parnell, S. R.; Men, Y.; Dalgliesh, R. M.; Eelkema, R.; Denkova, A. G. Ionizing Radiation-Induced Release from Poly(ε-Caprolactone-b-Ethylene Glycol) Micelles. *ACS Appl. Polym. Mater.* **2020**, *3*, 968–975.
15. Starkewolf, Z. B.; Miyachi, L.; Wong, J.; Guo, T. X-Ray Triggered Release of Doxorubicin from Nanoparticle Drug Carriers for Cancer Therapy. *Chem. Commun.* **2013**, *49*, 2545–2547.
16. Zhang, L.; Zhang, S.; Xu, J.; Li, Y.; He, J.; Yang, Y.; Huynh, T.; Ni, P.; Duan, G.; Yang, Z.; Zhou, R. Low-Dose X-Ray-Responsive Diselenide Nanocarriers for Effective Delivery of Anticancer Agents. *ACS Appl. Mater. Interfaces* **2020**, *12*, 43398–43407.
17. Zhou, Z.; Chan, A.; Wang, Z.; Huang, X.; Yu, G.; Jacobson, O.; Wang, S.; Liu, Y.; Shan, L.; Dai, Y.; Shen, Z.; Lin, L.; Chen, W.; Chen, X. Synchronous Chemoradiation Nanovesicles by X-Ray Triggered Cascade of Drug Release. *Angew. Chem. Int. Ed.* **2018**, *57*, 8463–8467.
18. Denkova, A. G.; Liu, H.; Men, Y.; Eelkema, R. Enhanced Cancer Therapy by Combining Radiation and Chemical Effects Mediated by Nanocarriers. *Adv. Ther.* **2020**, *3*, 1900177.
19. Li, H.; Luo, Q.; Zhang, H.; Ma, X.; Gu, Z.; Gong, Q.; Luo, K. Nanomedicine Embraces Cancer Radio-Immunotherapy: Mechanism, Design, Recent Advances, and Clinical Translation. *Chem. Soc. Rev.* **2023**, *52*, 47–96.
20. Pan, Y.; Tang, W.; Fan, W.; Zhang, J.; Chen, X. Development of Nanotechnology-Mediated Precision Radiotherapy for Anti-Metastasis and Radioprotection. *Chem. Soc. Rev.* **2022**, *51*, 9759–9830.
21. Son, S.; Kim, J.; Kim, J.; Kim, B.; Lee, J.; Kim, Y.; Li, M.; Kang, H.; Kim, J. S. Cancer Therapeutics Based on Diverse Energy Sources. *Chem. Soc. Rev.* **2022**, *51*, 8201–8215.
22. Cao, W.; Zhang, X.; Miao, X.; Yang, Z.; Xu, H. Gamma-Ray-Responsive Supramolecular Hydrogel Based on a Diselenide-Containing Polymer and a Peptide. *Angew. Chem. Int. Ed.* **2013**, *52*, 6233–6237.
23. Li, T.; Pan, S.; Zhuang, H.; Gao, S.; Xu, H. Selenium-Containing Carrier-Free Assemblies with Aggregation-Induced Emission Property Combine Cancer Radiotherapy with Chemotherapy. *ACS Appl. Bio Mater.* **2020**, *3*, 1283–1292.
24. Ma, N.; Xu, H.; An, L.; Li, J.; Sun, Z.; Zhang, X. Radiation-Sensitive Diselenide Block Co-Polymer Micellar Aggregates: Toward the Combination of Radiotherapy and Chemotherapy. *Langmuir* **2011**, *27*, 5874–5878.
25. Ding, Z.; Guo, Z.; Zheng, Y.; Wang, Z.; Fu, Q.; Liu, Z. Radiotherapy Reduces N-Oxides for Prodrug Activation in Tumors. *J. Am. Chem. Soc.* **2022**, *144*, 9458–9464.
26. Fu, Q.; Li, H.; Duan, D.; Wang, C.; Shen, S.; Ma, H.; Liu, Z. External-Radiation-Induced Local Hydroxylation Enables

DOI: 10.31635/ccschem.024.202303794
Citation: *CCS Chem.* **2024**, 6, 1712–1720
Link to VoR: https://doi.org/10.31635/ccschem.024.202303794

Remote Release of Functional Molecules in Tumors. *Angew. Chem. Int. Ed.* **2020**, *59*, 21546–21552.
27. Geng, J.; Zhang, Y.; Gao, Q.; Neumann, K.; Dong, H.; Porter, H.; Potter, M.; Ren, H.; Argyle, D.; Bradley, M. Switching on Prodrugs Using Radiotherapy. *Nat. Chem.* **2021**, *13*, 805–810.
28. Guo, Z.; Hong, H.; Zheng, Y.; Wang, Z.; Ding, Z.; Fu, Q.; Liu, Z. Radiotherapy-Induced Cleavage of Quaternary Ammonium Groups Activates Prodrugs in Tumors. *Angew. Chem. Int. Ed.* **2022**, *61*, e202205014.
29. Manikantan, K.; Khode, S.; Sayed, S. I.; Roe, J.; Nutting, C. M.; Rhys-Evans, P.; Harrington, K. J.; Kazi, R. Dysphagia in Head and Neck Cancer. *Cancer Treat Rev.* **2009**, *35*, 724–732.
30. Curran, W. J., Jr.; Paulus, R.; Langer, C. J.; Komaki, R.; Lee, J. S.; Hauser, S.; Movsas, B.; Wasserman, T.; Rosenthal, S. A.; Gore, E.; Machtay, M.; Sause, W.; Cox, J. D. Sequential vs. Concurrent Chemoradiation for Stage III Non-Small Cell Lung Cancer: Randomized Phase III Trial RTOG 9410. *J. Natl. Cancer Inst.* **2011**, *103*, 1452–1460.
31. De Ruysscher, D.; Niedermann, G.; Burnet, N. G.; Siva, S.; Lee, A. W. M.; Hegi-Johnson, F. Radiotherapy Toxicity. *Nat. Rev. Dis. Primers* **2019**, *5*, 13.
32. Ridouani, F.; Soliman, M. M.; England, R. W.; Hsu, M.; Moskowitz, C. S.; Doustaly, R.; Sofocleous, C. T.; Boas, F. E.; Yarmohammadi, H.; Deipolyi, A. R. Relationship of Radiation Dose to Efficacy of Radioembolization of Liver Metastasis from Breast Cancer. *Eur. J. Radiol.* **2021**, *136*, 109539.
33. Lawhn-Heath, C.; Hope, T. A.; Martinez, J.; Fung, E. K.; Shin, J.; Seo, Y.; Flavell, R. R. Dosimetry in Radionuclide Therapy: The Clinical Role of Measuring Radiation Dose. *Lancet Oncol.* **2022**, *23*, e75–e87.
34. Breve, T. G.; Filius, M.; Weerdenburg, S.; van der Griend, S. J.; Groeneveld, T. P.; Denkova, A. G.; Eelkema, R. Light-Sensitive Phenacyl Crosslinked Dextran Hydrogels for Controlled Delivery. *Chem. Eur. J.* **2022**, *28*, e202103523.
35. Yao, T.; Luthjens, L. H.; Gasparini, A.; Warman, J. M. A Study of Four Radiochromic Films Currently Used for (2D) Radiation Dosimetry. *Radiat. Phys. Chem.* **2017**, *133*, 37–44.
36. Schulte, J. W.; Suttle, J. F.; Wilhelm, R. Chemical Effects Produced in Chloroform by γ-Rays. *J. Am. Chem. Soc.* **1953**, *75*, 2222–2227.
37. Packer, J. E.; Willson, R. L.; Bahnemann, D.; Asmus, K. D. Electron-Transfer Reactions of Halogenated Aliphatic Peroxyl Radicals-Measurement of Absolute Rate Constants by Pulse-Radiolysis. *J. Chem. Soc., Perkin Trans. 2* **1980**, 296–299.
38. Abadie, M. J. M. Radiolysis of Liquid Chloroform in an Oxygen Free Atmosphere. *Radiat. Phys. Chem.* **1982**, *19*, 63–71.
39. Getoff, N. Decomposition of Biological Resistant Pollutants in Water by Irradiation. *Radiat. Phys. Chem.* **1990**, *35*, 432–439.
40. Rajesh, P.; LaVerne, J. A.; Pimblott, S. M. High Dose Radiolysis of Aqueous Solutions of Chloromethanes: Importance in the Storage of Radioactive Organic Wastes. *J. Nucl. Mater.* **2007**, *361*, 10–17.
41. Taghipour, F.; Evans, G. J. Radiolytic Dechlorination of Chlorinated Organics. *Radiat. Phys. Chem.* **1997**, *49*, 257–264.
42. Weber, L. W.; Boll, M.; Stampfl, A. Hepatotoxicity and Mechanism of Action of Haloalkanes: Carbon Tetrachloride as a Toxicological Model. *Crit. Rev. Toxicol.* **2003**, *33*, 105–136.

DOI: 10.31635/ccschem.024.202303794
Citation: *CCS Chem.* **2024**, 6, 1712–1720
Link to VoR: https://doi.org/10.31635/ccschem.024.202303794